THE JOURNAL OF PHYSICAL CHEMISTRY B

Article

Cite This: J. Phys. Chem. B 2018, 122, 4388−4396

pubs.acs.org/JPCB

Investigating the Secondary Structure of Membrane Peptides Utilizing Multiple ^{2}H-Labeled Hydrophobic Amino Acids via Electron Spin Echo Envelope Modulation (ESEEM) Spectroscopy

Lishan Liu, Indra D. Sahu, Lauren Bottorf, Robert M. McCarrick, and Gary A. Lorigan*

Department of Chemistry and Biochemistry, Miami University, Oxford, Ohio 45056, United States

Supporting Information

ABSTRACT: An electron spin echo envelope modulation (ESEEM) approach was used to probe local secondary structures of membrane proteins and peptides. This ESEEM method detects dipolar couplings between ^{2}H-labeled nuclei on the side chains of an amino acid (Leu or Val) and a strategically placed nitroxide spin-label in the proximity up to 8 Å. ESEEM spectra patterns for different samples correlate directly to the periodic structural feature of different secondary structures. Since this pattern can be affected by the side chain length and flexibility of the ^{2}H-labeled amino acid used in the experiment, it is important to examine several different hydrophobic amino acids (d_3 Ala, d_8 Val, d_8 Phe) utilizing this ESEEM approach. In this work, a series of ESEEM data were collected on the AChR M2δ membrane peptide to build a reference for the future application of this approach for various biological systems. The results indicate that, despite the relative intensity and signal-to-noise level, all amino acids share a similar ESEEM modulation pattern for α-helical structures. Thus, all commercially available ^{2}H-labeled hydrophobic amino acids can be utilized as probes for the further application of this ESEEM approach. Also, the ESEEM signal intensities increase as the side chain length gets longer or less rigid. In addition, longer side chain amino acids had a larger ^{2}H ESEEM FT peak centered at the ^{2}H Larmor frequency for the $i \pm 4$ sample when compared to the corresponding $i \pm 3$ sample. For shorter side chain amino acids, the ^{2}H ESEEM FT peak intensity ratio between $i \pm 4$ and $i \pm 3$ was not well-defined.

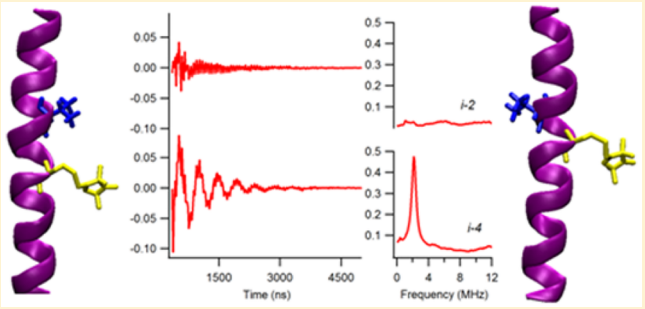

INTRODUCTION

Previously, we reported a very efficient and straightforward local secondary structure determination approach utilizing the pulsed EPR technique electron spin echo envelope modulation (ESEEM).[1−7] ESEEM spectroscopy is a very powerful pulsed EPR spectroscopic technique and has been applied to study several different biological systems.[8−13] The local secondary structure of membrane-spanning or membrane-associated proteins and peptides can be identified by detecting weak dipolar couplings between ^{2}H atoms in a ^{2}H-labeled amino acid side chain and a nearby spin label. This method requires μg amounts of protein sample, a couple hours of data acquisition time, and a minimum amount of data analysis. Also, this method has no size limitation for the protein complexes of interest and can be conducted in their native mimetic environments.

Figure 1 shows the spin-labeling and ^{2}H-labeling strategies of this ESEEM approach. A cysteine mutated nitroxide spin label (yellow) is positioned strategically one, two, three, and four residues away from an amino acid (blue) with a deuterated side chain (denoted as $i \pm 1$ to $i \pm 4$). The characteristic periodicity of the α-helix or β-strand structure reveals unique patterns in individual ESEEM spectra.[2] For a typical α-helix, the ^{2}H-labeled side chain and the spin label for $i \pm 3$ and $i \pm 4$ samples are located on the same side of the helix, as shown in Figure 1A. Thus, weak dipolar couplings between the ^{2}H-labeled side chain and the spin label can be detected by the ESEEM technique for $i \pm 3$ and $i \pm 4$ samples. However, the distance between the ^{2}H-labeled side chain and the spin label is more than 8 Å for $i \pm 1$ and $i \pm 2$ samples, as they point to opposite sides of the helix (Figure 1B). Thus, no ^{2}H modulation can be observed for $i \pm 1$ and $i \pm 2$ samples. More experiments have been performed with ^{2}H-labeled d_{10} Leu to build up a library of references for further applications of this method. The long and flexible side chain of Leu gives rise to several unique features within different ESEEM spectra. The ESEEM data always show strong ^{2}H modulation in the ESEEM time domain data and a high intensity ^{2}H FT peak in the frequency domain data for $i \pm 4$ and $i \pm 3$ samples. In addition, ^{2}H modulation of $i \pm 4$ samples was always significantly deeper than the corresponding $i \pm 3$ sample.

In order to apply this approach to different biological systems with a variety of different types of amino acid compositions, it is important to examine the effects of side chain length and

Received: December 1, 2017
Revised: April 3, 2018
Published: April 3, 2018

DOI: 10.1021/acs.jpcb.7b11890
J. Phys. Chem. B 2018, 122, 4388−4396

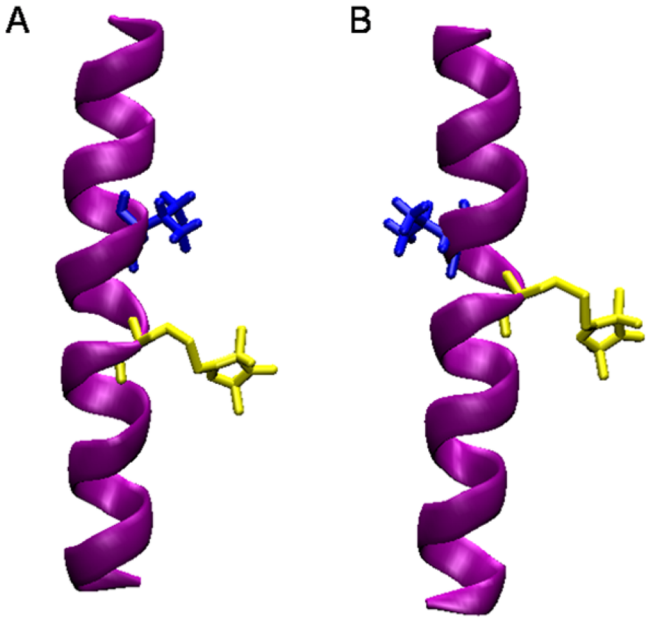

Figure 1. ESEEM experiment SDSL and isotopic label paradigm with a model α-helix (AChR M2δ peptide in purple) for (A) $i \pm 3$ and $i \pm 4$ samples and (B) $i \pm 1$ and $i \pm 2$ samples. ^{2}H-Labeled d_8 Val residues are highlighted in blue at position 9. Cys residues attached with MTSL are highlighted in yellow.

flexibility on α-helical ESEEM spectral patterns. In this paper, three Ala, two Val, and one Phe within the AChR M2δ peptide were mapped out on both N-terminal (−) and C-terminal (+) sides with this ESEEM approach. Experimental results show that commercially available ^{2}H-labeled hydrophobic amino acids (d_3 Ala, d_8 Val, d_8 Phe, d_{10} Leu) share a similar ESEEM spectral pattern for an α-helix. Thus, all of these ^{2}H-labeled residues can be used to identify α-helical secondary structural components within membrane proteins and peptides. In addition, this study shows that side chain length and flexibility can affect the signal-to-noise ratio and relative modulation amplitude. In general, ^{2}H-labeled amino acids with longer side chains and more deuterium atoms give rise to a deeper modulation depth. Also, ESEEM results obtained with amino acids with longer side chains, such as d_8 Phe and d_{10} Leu, always show a larger ^{2}H ESEEM FT peak for $i \pm 4$ samples, when compared to the corresponding $i \pm 3$ sample. However, short side chain amino acids (such as d_3 Ala) do not share this ESEEM pattern. The ESEEM pattern of ^{2}H-labeled amino acids with long side chains can potentially be utilized to identify other helical structures such as a π-helix and a 3_{10}-helix.[14]

EXPERIMENTAL METHODS

The M2δ peptide of the nicotinic acetylcholine receptor (AChR) with 23 amino acid residues was used as an α-helical structural model for transmembrane peptides and proteins (denoted as AChR M2δ).[15−17] Table 1 shows the amino acid sequence of the wild type and all experimental constructs of the M2δ peptide. There are three Ala residues at positions 6, 12, and 14; two Val residues at positions 9 and 15; and one Phe residue at position 16. Four different peptides were designed for both the left (−) and right (+) sides of each of these residues. The ^{2}H-labeled amino acids (d_3 Ala, d_8 Val, or d_8 Phe) are highlighted in bold red (i). Cysteine is highlighted in blue at four successive positions (denoted as $i + 1$ to $i + 4$) for spin label attachment.

Table 1. Wild Type and Experimental Constructs of AChR M2δ (α-Helix)[a]

	N-terminal (-)	C-terminal (+)
Wide Type	NH_2-EKMSTAISVLLAQAVFLLLTSQR-COOH	
Ala6	NH_2-EKMSCAISVLLAQAVFLLLTSQR-COOH	NH_2-EKMSTACSVLLAQAVFLLLTSQR-COOH
	NH_2-EKMCTAISVLLAQAVFLLLTSQR-COOH	NH_2-EKMSTAICVLLAQAVFLLLTSQR-COOH
	NH_2-EKCSTAISVLLAQAVFLLLTSQR-COOH	NH_2-EKMSTAISCLLAQAVFLLLTSQR-COOH
	NH_2-ECMSTAISVLLAQAVFLLLTSQR-COOH	NH_2-EKMSTAISVCLAQAVFLLLTSQR-COOH
Ala12	NH_2-EKMSTAISVLCAQAVFLLLTSQR-COOH	NH_2-EKMSTAISVLLACAVFLLLTSQR-COOH
	NH_2-EKMSTAISVCLAQAVFLLLTSQR-COOH	NH_2-EKMSTAISVLLAQCVFLLLTSQR-COOH
	NH_2-EKMSTAISCLLAQAVFLLLTSQR-COOH	NH_2-EKMSTAISVLLAQACFLLLTSQR-COOH
	NH_2-EKMSTAICVLLAQAVFLLLTSQR-COOH	NH_2-EKMSTAISVLLAQAVCLLLTSQR-COOH
Ala14	NH_2-EKMSTAISVLLACAVFLLLTSQR-COOH	NH_2-EKMSTAISVLLAQACFLLLTSQR-COOH
	NH_2-EKMSTAISVLLCQAVFLLLTSQR-COOH	NH_2-EKMSTAISVLLAQAVCLLLTSQR-COOH
	NH_2-EKMSTAISVLCAQAVFLLLTSQR-COOH	NH_2-EKMSTAISVLLAQAVFCLLTSQR-COOH
	NH_2-EKMSTAISVCLAQAVFLLLTSQR-COOH	NH_2-EKMSTAISVLLAQAVFLCLTSQR-COOH
Val9	NH_2-EKMSTAICVLLAQAVFLLLTSQR-COOH	NH_2-EKMSTAISVCLAQAVFLLLTSQR-COOH
	NH_2-EKMSTACSVLLAQAVFLLLTSQR-COOH	NH_2-EKMSTAISVLCAQAVFLLLTSQR-COOH
	NH_2-EKMSTCISVLLAQAVFLLLTSQR-COOH	NH_2-EKMSTAISVLLCQAVFLLLTSQR-COOH
	NH_2-EKMSCAISVLLAQAVFLLLTSQR-COOH	NH_2-EKMSTAISVLLACAVFLLLTSQR-COOH
Val15	NH_2-EKMSTAISVLLAQCVFLLLTSQR-COOH	NH_2-EKMSTAISVLLAQAVCLLLTSQR-COOH
	NH_2-EKMSTAISVLLACAVFLLLTSQR-COOH	NH_2-EKMSTAISVLLAQAVFCLLTSQR-COOH
	NH_2-EKMSTAISVLLCQAVFLLLTSQR-COOH	NH_2-EKMSTAISVLLAQAVFLCLTSQR-COOH
	NH_2-EKMSTAISVLCAQAVFLLLTSQR-COOH	NH_2-EKMSTAISVLLAQAVFLLCTSQR-COOH
Phe16	NH_2-EKMSTAISVLLAQACFLLLTSQR-COOH	NH_2-EKMSTAISVLLAQAVFCLLTSQR-COOH
	NH_2-EKMSTAISVLLAQCVFLLLTSQR-COOH	NH_2-EKMSTAISVLLAQAVFLCLTSQR-COOH
	NH_2-EKMSTAISVLLACAVFLLLTSQR-COOH	NH_2-EKMSTAISVLLAQAVFLLCTSQR-COOH
	NH_2-EKMSTAISVLLCQAVFLLLTSQR-COOH	NH_2-EKMSTAISVLLAQAVFLLLCSQR-COOH

[a] ^{2}H-labeled d_3 Ala, d_8 Val, and d_8 Phe are marked in bold red. The blue bold C's mark the positions where the amino acid is replaced by Cys for MTSL incorporation.

DOI: 10.1021/acs.jpcb.7b11890
J. Phys. Chem. B 2018, 122, 4388−4396

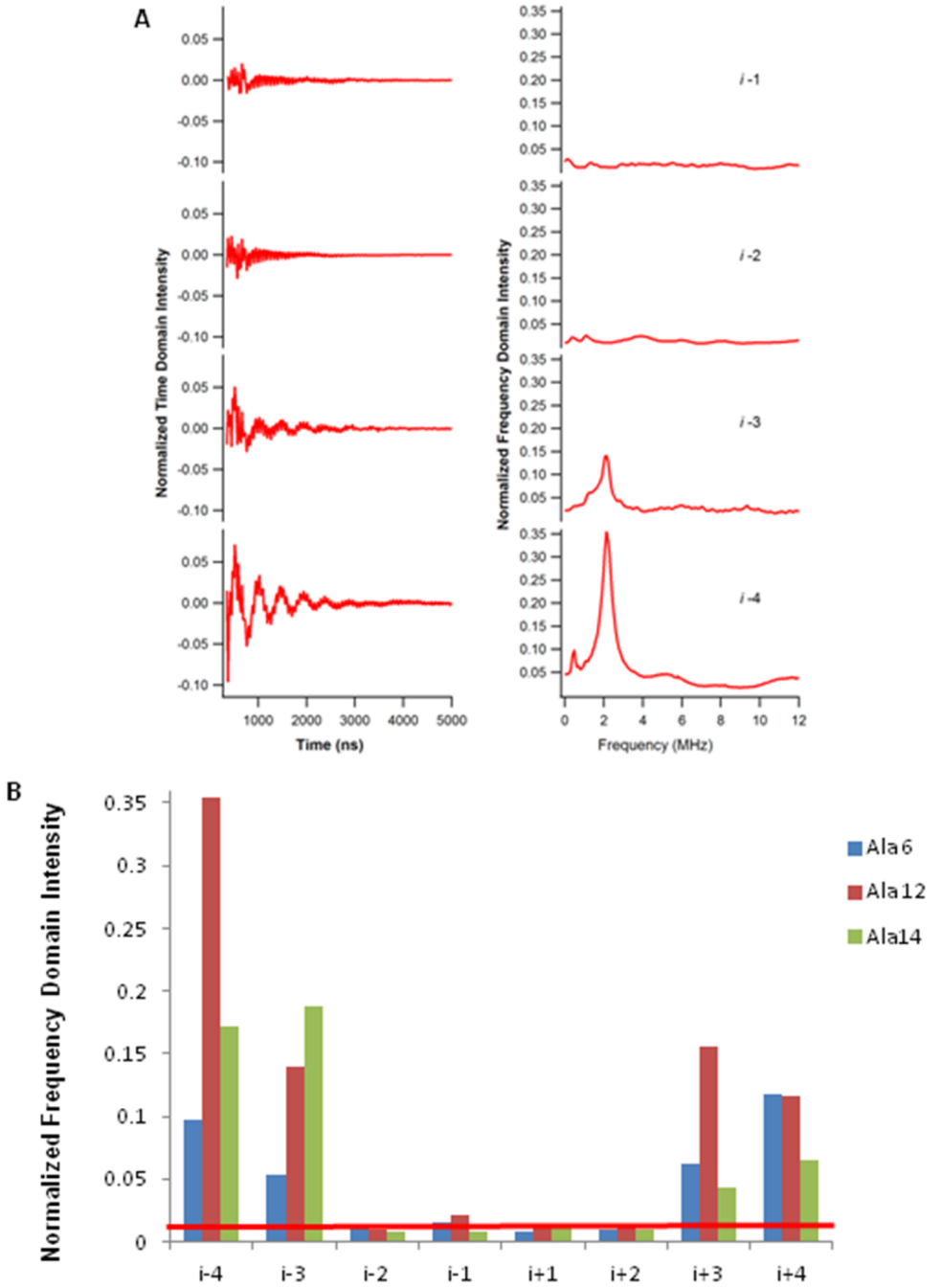

Figure 2. (A) Three-pulse ESEEM experimental data of AChR M2δ with ^{2}H-labeled d_3 Ala12 on the N-terminal side in DMPC/DHPC (3.5:1) bicelles at τ = 200 ns for the $i-1$ to $i-4$ in (left) time domain and (right) frequency domain. (B) Normalized frequency domain intensity from all three ESEEM data sets for ^{2}H-labeled d_3 Ala on both the N-terminal and C-terminal sides.

All peptides were synthesized on a CEM liberty solid-phase peptide synthesizer utilizing Fmoc chemistry.[18−20] Full-length AChR M2δ peptides were cleaved from the solid support and purified using reverse-phase HPLC as described.[3,4,21,22] Purified peptides were labeled with a 5-fold excess of MTSL (Toronto Research Chemicals) in DMSO for 20 h, and excess MTSL was removed by HPLC. MALDI-TOF was utilized to confirm the molecular weight and purities of the target AChR M2δ peptides. HPLC fractions for pure and labeled peptides were lyophilized to powder form for further use and storage.

For these experiments, bicelles were used as the membrane mimic system to yield high quality ESEEM data.[1] MTSL-labeled M2δ peptides were integrated into 1,2-dimyristoyl-*sn*-glycero-3-phosphocholine/1,2-dihexanoyl-*sn*-glycero-3-phosphocholine (DMPC/DHPC) bicelles (q = 3.5/1) at 1:1000 peptide to lipid molar ratio. X-Band CW-EPR (∼9 GHz) spectroscopy was used to measure the spin concentrations (∼150 μM) of all bicelle samples.

Three-pulse ESEEM measurements were performed on a Bruker ELEXSYS E580 instrument with an ER 4118X MS3 resonator using a 200 ns tau value with a microwave frequency of ∼9.269 GHz at 80 K. For all samples, a starting T of 386 ns and 512 points in 12 ns increments were used to collect the spectra. All ESEEM data were obtained with 40 μL of bicelle samples and averaged with 30 scans.

DOI: 10.1021/acs.jpcb.7b11890
J. Phys. Chem. B 2018, 122, 4388−4396

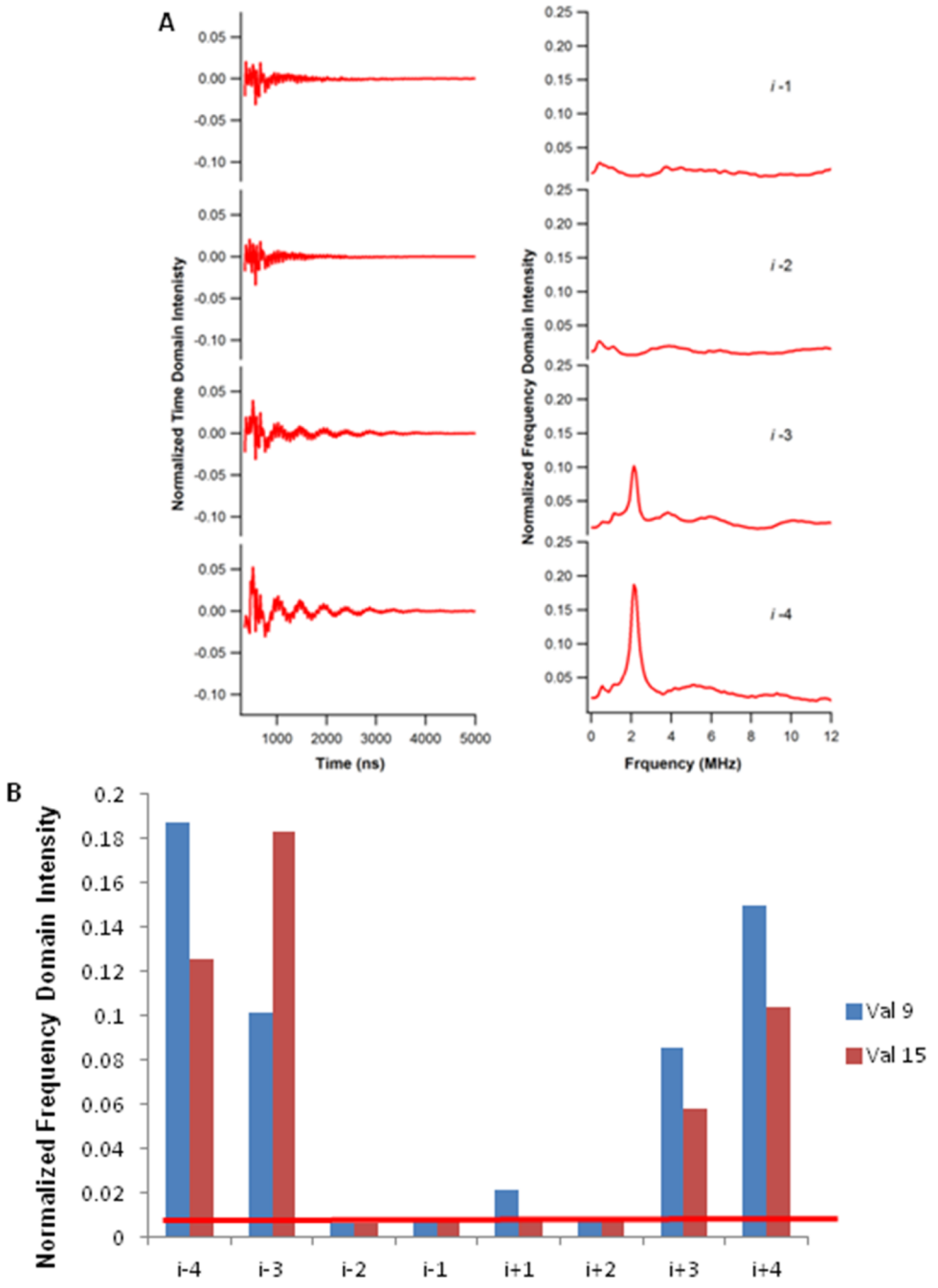

Figure 3. (A) Three-pulse ESEEM experimental data of AChR M2δ with ^{2}H-labeled d_8 Val9 on the N-terminal side in DMPC/DHPC (3.5:1) bicelles at τ = 200 ns for the $i-1$ to $i-4$ in (left) time domain and (right) frequency domain. (B) Normalized frequency domain intensity from both ESEEM data sets for ^{2}H-labeled d_8 Val on both the N-terminal and C-terminal sides.

The original ESEEM time domain data were normalized by division through a polynomial fit, followed by subtraction of unity, as suggested previously.[6,23−25] The missing data points were obtained via a back-prediction using the LPSVP algorithm.[26] The data were further processed by Hamming apodization and zero filling.[8] A cross-term averaged Fourier transformation (FT) was performed on the resulting spectrum to generate the corresponding frequency domain with minimized artifacts.[6] The maximum intensity of the deuterium peak at 2.3 MHz was measured, and peak intensity was recorded for further analysis.

RESULTS

Three hydrophobic amino acids with different side chains (^{2}H-labeled d_3 Ala, ^{2}H-labeled d_8 Val, and ^{2}H-labeled d_8 Phe) were utilized as ^{2}H-labeled probes for this ESEEM secondary structure determination method. Experimental results obtained from this study were presented and compared to previously reported ^{2}H-labeled d_{10} Leu data.

Figure 2 shows three-pulse ESEEM secondary structural data for the AChR M2δ peptide utilizing ^{2}H-labeled d_3 Ala as the ^{2}H-labeled probe. ESEEM time and frequency domain data for the ^{2}H-labeled d_3 Ala12 on the N-terminal side (−) are shown in Figure 2A. ^{2}H modulation is clearly seen in the time domain

DOI: 10.1021/acs.jpcb.7b11890
J. Phys. Chem. B 2018, 122, 4388−4396

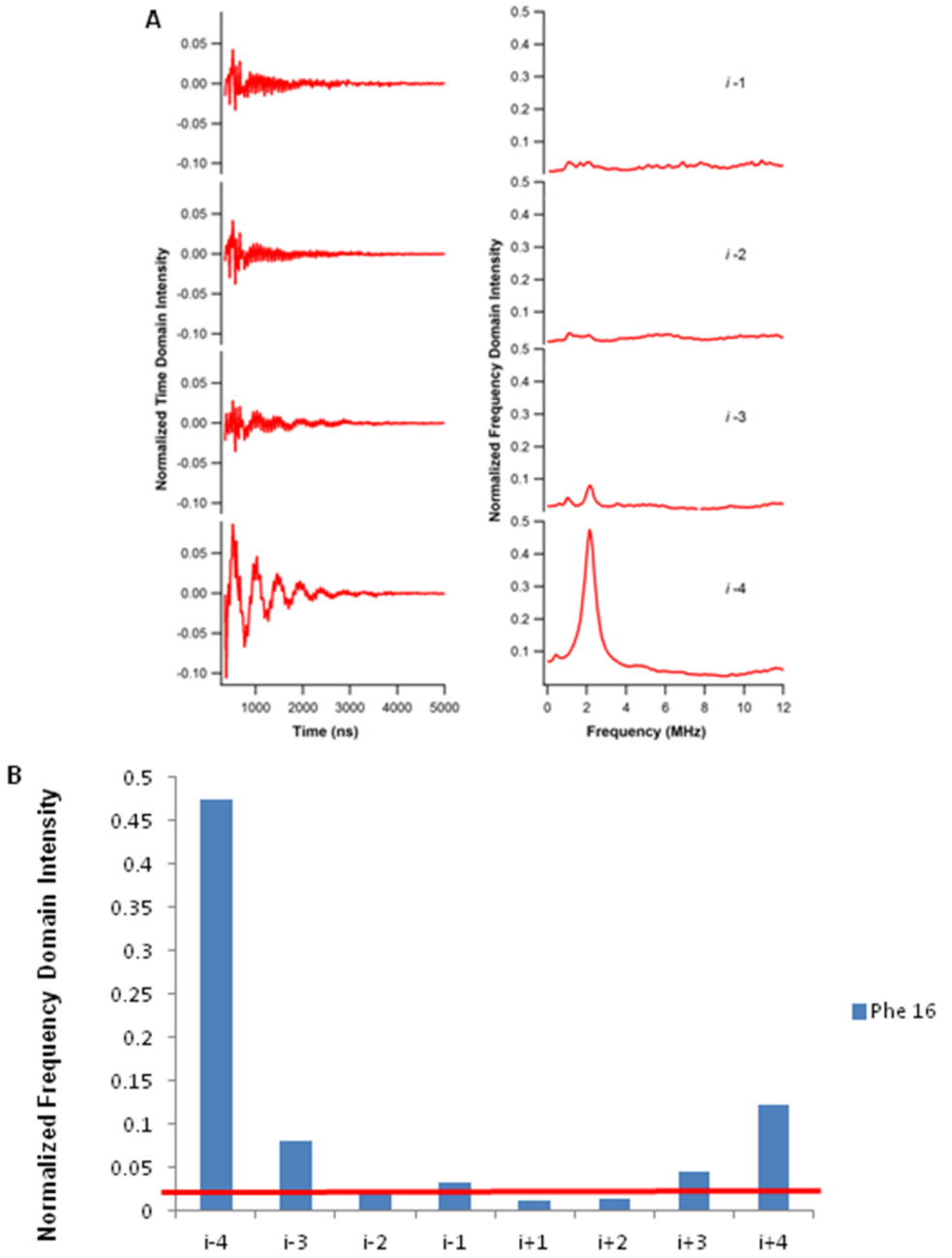

Figure 4. (A) Three-pulse ESEEM experimental data of AChR M2δ with ^{2}H-labeled d_8 Phe16 on the N-terminal side in DMPC/DHPC (3.5:1) bicelles at τ = 200 ns for the $i-1$ to $i-4$ in (left) time domain and (right) frequency domain. (B) Normalized frequency domain intensity from the ESEEM data set for ^{2}H-labeled d_8 Phe16 on both the N-terminal and C-terminal sides.

data of the $i-3$ and $i-4$ samples (left panel). Correspondingly, a peak centered at the ^{2}H Larmor frequency can be observed in the frequency domain data for both samples (right panel). ^{2}H modulation was not observed for both the $i-1$ and $i-2$ samples. This pattern was consistent with the previously established ESEEM signature of an α-helical structure.[1,3] All six sets of ESEEM data for ^{2}H-labeled d_3 Ala showed similar patterns (see Figures S1–S3 in the Supporting Information). Normalized frequency domain ^{2}H FT peak intensities were measured and plotted in Figure 2B. ESEEM ^{2}H peak intensities varied from 0.01 to 0.36. Variations in FT peak intensities of the ^{2}H modulation at those different positions were smaller when compared to Leu data.[3] However, any sample with an obvious ESEEM FT ^{2}H peak has a FT peak intensity above the 0.01 level which is indicated by the red line.

Previously, ^{2}H-labeled d_8 Val was used to demonstrate the feasibility of this ESEEM secondary structure approach.[1] Here, two Val residues at positions 9 and 15 were mapped out on both the N-terminal and C-terminal sides (see Figures S4 and S5 in the Supporting Information) to get a better understanding of this ^{2}H-labeled probe. Figure 3A shows the ESEEM time domain (left panel) and frequency domain (right panel) data for ^{2}H-labeled d_8 Val9 on the N-terminal side (−). It shows a similar α-helical pattern that ^{2}H modulation is observed for $i-3$ and $i-4$ samples but not for $i-1$ or $i-2$ samples. Normalized ^{2}H peak intensities were plotted in

DOI: 10.1021/acs.jpcb.7b11890
J. Phys. Chem. B 2018, 122, 4388−4396

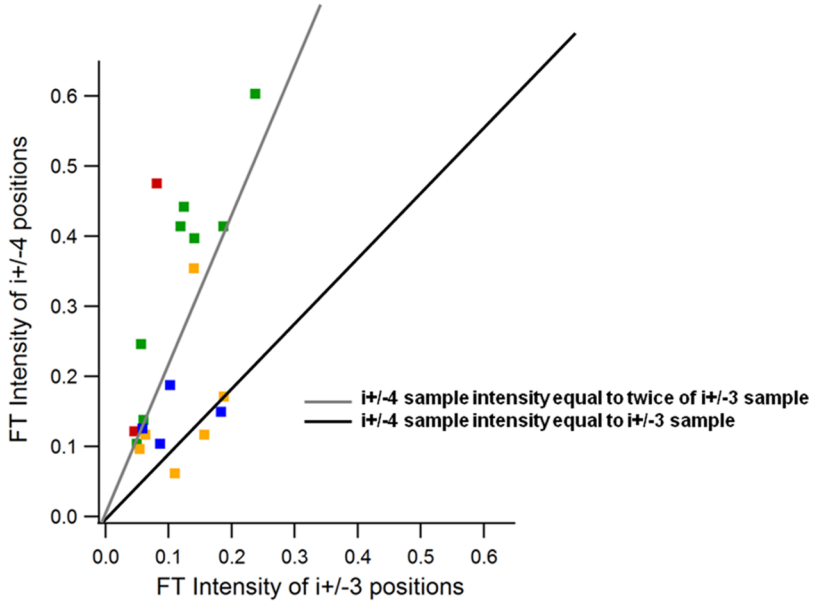

Figure 5. Frequency domain ^{2}H peak intensity comparison between $i \pm 4$ positions and $i \pm 3$ positions for ^{2}H-labeled d_3 Ala (yellow), ^{2}H-labeled d_8 Val (blue), ^{2}H-labeled d_8 Phe (red), and ^{2}H-labeled d_{10} Leu (green). The black line represents that the ESEEM ^{2}H FT peak intensity of the $i \pm 4$ sample is equal to that of the $i \pm 3$ sample. The gray line represents the ESEEM ^{2}H FT peak intensity of the $i \pm 4$ sample is twice that of the corresponding $i \pm 3$ sample.

Figure 3B. ^{2}H-Labeled d_8 Val9 and Val15 ESEEM ^{2}H peak intensities varied from 0.01 to 0.19.

Figure 4 shows ESEEM data for ^{2}H-labeled d_8 Phe16. The normalized ESEEM time (left panel) and frequency domain (right panel) data of ^{2}H-labeled d_8 Phe16 on the N-terminal side (−) are shown in Figure 4A. A similar ESEEM pattern for the α-helix was observed. Figure 4B shows the frequency domain ^{2}H ESEEM FT peak intensities for ^{2}H-labeled d_8 Phe16 for both N-terminal and C-terminal sides (see Figure S6 for remaining ESEEM data). ^{2}H-Labeled d_8 Phe 16 ESEEM ^{2}H peak intensities varied from 0.02 to 0.48. The minor peaks below 2 MHz observed in frequency domain data probably are an artifact and may be arising from data collection and poor sample quality. The relative ^{2}H peak intensities are not affected by these artifacts.

Normalized frequency domain ^{2}H peak FT intensities of Ala, Val, and Phe at $i \pm 3$ and $i \pm 4$ positions were combined with previous Leu data and plotted in Figure 5. The black solid line represents equal ^{2}H FT peak intensities at $i \pm 4$ and $i \pm 3$ positions, whereas the gray line is indicative of the $i \pm 4$ FT ^{2}H peak twice as large as the corresponding $i \pm 3$ peak. The graph clearly shows that the $i \pm 4$ sample intensities are at least twice as large as those of the corresponding $i \pm 3$ samples for ^{2}H-labeled amino acid probes with longer side chains (d_8 Phe and d_{10} Leu). All data points from long side chain amino acids were spotted near or above the gray line. Data points for ^{2}H-labeled amino acid probes with shorter side chains (d_3 Ala and d_8 Val) were mainly found around the black line with a smaller FT peak intensity. Also, it was noticed that the longer the side chain, the further away the data point was from zero point which indicates the longer side chain leads to a higher ESEEM signal intensity in general. Since amino acids with longer side chains are more flexible to adapt different conformations, it was also observed that the ^{2}H-labeled amino acid probes with longer side chain length yield more scattered data points.

DISCUSSION

Four different ^{2}H-labeled amino acids have been examined with this ESEEM secondary structure determination approach. The side chains of ^{2}H-labeled amino acids and spin-labeled MTSL used in this study are shown in Figure 6A.

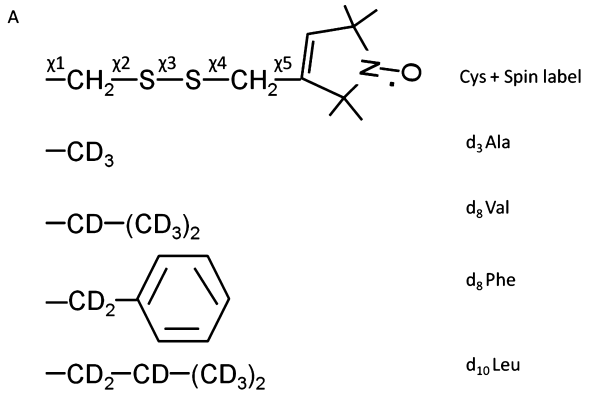

Figure 6. (A) Side chains of MTSL-labeled cysteine, ^{2}H-labeled d_3 Ala, ^{2}H-labeled d_8 Val, ^{2}H-labeled d_8 Phe, and ^{2}H-labeled d_{10} Leu. (B) Position of ^{2}H-labeled amino acids within the amino acid sequence of AChR M2δ peptide highlighted in **bold**.

Multiple ^{2}H-Labeled Hydrophobic Amino Acids Can Be Utilized as Probes to Indentify α-Helical Secondary Structure with This ESEEM Approach. We used four different ^{2}H-labeled hydrophobic amino acids as probes for this ESEEM approach to study the secondary structure of an α-helical peptide. For the AChR M2δ transmembrane peptide, weak dipolar couplings between ^{2}H atoms on the amino acid side chain and the spin label were detected for $i \pm 3$ and $i \pm 4$ samples. However, no ^{2}H modulation was observed for any of

DOI: 10.1021/acs.jpcb.7b11890
J. Phys. Chem. B 2018, 122, 4388−4396

the $i \pm 2$ samples. Also, ^{2}H modulation amplitudes for $i \pm 1$ samples are around noise level and significantly smaller than those for the corresponding $i \pm 3$ and $i \pm 4$ samples. For any frequency domain data with an obvious ^{2}H FT peak, normalized ^{2}H FT peak intensities at ^{2}H Larmor frequency are larger than 0.02.

Side Chain Lengths of Different Amino Acids Have Effects on the ESEEM Signal. Figure 6 shows side chains of ^{2}H-labeled amino acids and the MTSL-labeled cysteine side chain (R_1). As shown in Figure 6A, the MTSL-labeled cysteine side chain is longer and flexible with three torsion angle rotations about χ1, χ2, and χ3 and two additional free torsion angle rotations about χ4 and χ5.[27−30] The ^{2}H-labeled amino acids used in this study have a varying number of deuterium atoms and degrees of freedom on the side chain torsion angle rotations. The favorable conformation of the side chain can be altered by the dynamics and the tertiary interactions with the environment. In general, as the side chain of ^{2}H-labeled amino acids gets longer, the number of deuterium atoms on the side chain increases. In addition, additional C−C bonds on longer side chain amino acids bring deuteron atoms closer to the N−O nitroxide bond. Thus, ^{2}H-labeled amino acids with a longer side chain (such as d_8 Phe and d_{10} Leu) have the ability to give deeper ^{2}H modulation in ESEEM spectra when compared to shorter side chain amino acids (such as d_3 Ala). However, more degrees of freedom on the side chain torsion angle rotations for longer side chain amino acids increases the number of different conformations that can be adopted.[31,32] Thus, the ESEEM modulation depth of longer side chain amino acids has a larger variation when compared to short side chain amino acids, such as Ala.

Previously, we demonstrated that $i \pm 4$ samples for ^{2}H-labeled d_{10} Leu always have deeper ^{2}H modulation when compared to the corresponding $i \pm 3$ positions.[3,4,6,7,14] ESEEM data from ^{2}H-labeled d_8 Phe showed the same pattern (Figure 4). Since a standard α-helix has a 3.6 amino acid per turn regularity, the angle between the side chain of the amino acid and the MTSL with respect to the helical axis was smaller in $i \pm 4$ positions than $i \pm 3$ positions.[27,33,34] As the side chain gets longer, the distance between ^{2}H atoms on the ^{2}H-labeled amino acid side chain and the nitroxide spin label reflects these angle differences more significantly. However, this angular difference between $i \pm 4$ and $i \pm 3$ samples cannot be resolved with short side chain amino acids from the ESEEM data.

Variation of ^{2}H Modulation Depth Was Consistent with the Kinked Model of the AChR M2δ Peptide. Previously, cyro-EM, computer MD simulations, and MAS solid-state NMR studies suggested that there is a kink on the AChR M2δ peptide around the Leu11 position.[35,36] In addition, we mapped out the AChR M2δ peptide with four Leu residues via this ESEEM approach. Our experimental results are consistent with a kinked model of AChR near the Leu11 position. The variation of distances between ^{2}H-labeled amino acid side chains and spin labels suggests that conformations of these amino acid side chains and the peptide backbone adapted were consistent with this kinked α-helical model of M2δ in a lipid bilayer. Enhanced ^{2}H FT peaks were observed for Leu10 on both sides, especially for the ^{2}H-labeled d_{10} Leu10 $i \pm 4$ samples. Those results indicated the distances between side chains of Leu10 and the side chain of residues at positions 6 or 14 are closer when compared to other $i \pm 4$ samples.

In the current study, the ESEEM modulation depth was consistent with these results. The same enhanced ^{2}H FT peak was observed for the same position as Ala6 $i + 4$ and Ala14 $i - 4$ samples. These results are consistent with a kink-induced proximity around the Leu11 position. In a DMPC bilayer, the ESEEM data showed a closer distance between side chains at positions 6 and 10 or positions 10 and 14, which suggested amino acids reside in the inner circle of a kink. In addition, ^{2}H modulation on the N-terminal side of Phe16 was much larger than the C-terminal side, which is consistent with a kink induced burial of the charged residue.[35] The ^{2}H FT signal on the N-terminal side (−) of Phe16 was significantly larger than the C-terminal side (+). This suggests that the Phe16 side chain was closer toward amino acid side chains on the N-terminal side of the peptide. The thermodynamic cost of transferring a polar or charged residue such as Gln13 into the hydrophobic core of the lipid bilayer is high.[37] Former studies have shown that, in a kinked model of the AChR M2δ peptide, a long amino acid side chain such as Phe16 is closer and parallel to the side chain of Gln13.[38] As a result, the carbonyl group of the Gln13 side chain was partially buried by the aromatic ring of the Phe16 side chain.[38,39] This kink-induced electrostatic burial of Gln13 is consistent with the ESEEM data from ^{2}H-labeled d_8 Phe16. However, the kinked model of AChR M2δ peptide could be highly lipid composition and liposome architecture dependent.[17,35]

CONCLUSION

In conclusion, the current and previous results demonstrated a complete picture of utilizing ESEEM and SDSL to identify α-helical secondary structural components with several different commercially available ^{2}H-labeled hydrophobic amino acids. This ESEEM approach identified different secondary structures through the patterns of distances between a ^{2}H-labeled amino acid side chain to a nitroxide spin label placed in its vicinity.[1−3] In general, ^{2}H modulation can be observed for $i \pm 3$ and $i \pm 4$ positions for an α-helix but not for $i \pm 1$ or $i \pm 2$ positions. When utilizing different ^{2}H-labeled amino acids with various side chain lengths and flexibilities, this pattern still applied, while the absolute and relative ESEEM ^{2}H peak intensities varied. In addition, the signal intensities of different positions along the AChR M2δ peptide vary in a fashion which was consistent with a kinked model for the M2δ peptide. Moreover, the ESEEM ^{2}H FT peak amplitude and intensity variation at $i \pm 3$ and $i \pm 4$ positions increased as the side chain length increased. In addition, longer side chain amino acids such as d_8 Phe and d_{10} Leu showed more intense $i \pm 4$ ^{2}H peaks than the corresponding $i \pm 3$ peaks. Further studies should be performed to investigate the ESEEM pattern with long side chain amino acids using different helical structures such as a π- or 3_{10}-helices.

This ESEEM approach required a small amount of protein sample (40 μL with μmol concentration) and a couple hours of data acquisition time and can be used to study systems with no size limitation.[1−3] With those specific signal patterns established for an α-helix with different amino acid probes, this approach now can be applied widely to biological systems with various amino acid compositions which are inherently difficult to study with traditional biophysical methods.

DOI: 10.1021/acs.jpcb.7b11890
J. Phys. Chem. B 2018, 122, 4388−4396

■ ASSOCIATED CONTENT

Supporting Information

The Supporting Information is available free of charge on the ACS Publications website at DOI: 10.1021/acs.jpcb.7b11890.

Six sets of three-pulse ESEEM data for ^{2}H-labeled d_3 Ala (Figures S1−S3), two sets of three-pulse ESEEM data for ^{2}H-labeled d_3 Val (Figures S4−S5), and one set of three-pulse ESEEM data for ^{2}H-labeled d_3 Phe (Figure S6) (PDF)

■ AUTHOR INFORMATION

Corresponding Author

*E-mail: gary.lorigan@miamioh.edu. Phone: 513-529-3338.

ORCID

Gary A. Lorigan: 0000-0002-2395-3459

Notes

The authors declare no competing financial interest.

■ ACKNOWLEDGMENTS

This work was generously supported by a NIGMS/NIH Maximizing Investigator's Research Award (MIRA) R35 GM126935 award and a NSF CHE-1807131 grant. The pulsed EPR spectrometer was purchased through funding provided by the NSF (MRI-1725502), the Ohio Board of Reagents, and Miami University. Gary A. Lorigan would also like to acknowledge support from the John W. Steube Professorship.

■ REFERENCES

(1) Mayo, D.; Zhou, A.; Sahu, I.; McCarrick, R.; Walton, P.; Ring, A.; Troxel, K.; Coey, A.; Hawn, J.; Emwas, A. H.; Lorigan, G. A. Probing the structure of membrane proteins with electron spin echo envelope modulation spectroscopy. *Protein Sci.* **2011**, *20*, 1100−1104.

(2) Zhou, A.; Abu-Baker, S.; Sahu, I. D.; Liu, L.; McCarrick, R. M.; Dabney-Smith, C.; Lorigan, G. A. Determining α-helical and β-sheet secondary structures via pulsed electron spin resonance spectroscopy. *Biochemistry* **2012**, *51*, 7417−7419.

(3) Liu, L.; Sahu, I. D.; Mayo, D. J.; McCarrick, R. M.; Troxel, K.; Zhou, A.; Shockley, E.; Lorigan, G. A. Enhancement of electron spin echo envelope modulation spectroscopic methods to investigate the secondary structure of membrane proteins. *J. Phys. Chem. B* **2012**, *116*, 11041−11045.

(4) Liu, L.; Mayo, D. J.; Sahu, I. D.; Zhou, A.; Zhang, R.; McCarrick, R. M.; Lorigan, G. A. Determining the secondary structure of membrane proteins and peptides via electron spin echo envelope modulation (ESEEM) spectroscopy. *Methods Enzymol.* **2015**, *564*, 289−313.

(5) Zhang, R.; Sahu, I. D.; Gibson, K. R.; Muhammad, N.; Bali, A. P.; Comer, R. G.; Liu, L.; Craig, A. F.; McCarrick, R. M.; Dabney-Smith, C.; Sanders, C. R.; Lorigan, G. A. Development of electron spin echo envelope modulation (ESEEM) spectroscopy to probe the secondary structure of recomninant membrane proteins in lipid bilayer. *Protein Sci.* **2015**, *24*, 1707−1713.

(6) Liu, L.; Hess, J.; Sahu, I. D.; FitzGerald, P. G.; McCarrick, R. M. Probing the local secondary structure of human vimentin with electron spin echo envelope modulation (ESEEM) spectroscopy. *J. Phys. Chem. B* **2016**, *120*, 12321−12326.

(7) Liu, L.; Sahu, I. D.; McCarrick, R. M.; Lorigan, G. Probing the secondary structure of membrane peptides using 2h-labeled d10 leucine via site-directing spin-labeling (SDSL) and electron spin echo envelope modulation (ESEEM) spectroscopy. *J. Phys. Chem. B* **2016**, *120*, 633−640.

(8) Cieslak, J. A.; Focia, P. J.; Gross, A. Electron spin-echo envelope modulation (ESEEM) reveals water and phosphate interactions with the KcsA potassium channel. *Biochemistry* **2010**, *49*, 1486−1494.

(9) Volkov, A.; Dockter, C.; Polyhach, Y.; Paulsen, H.; Jeschke, G. Site-specific information on membrane protein folding by electron spin echo envelope modulation spectroscopy. *J. Phys. Chem. Lett.* **2010**, *1*, 663−667.

(10) Gordon-Grossman, M.; Zimmermann, H.; Wolf, S. G.; Shai, Y.; Goldfarb, D. Investigation of model membrane disruption mechanism by melittin using pulse electron paramagnetic resonance spectroscopy and cryogenic transmission electron microscopy. *J. Phys. Chem. B* **2012**, *116*, 179−188.

(11) Syryamina, V. N.; Maryasov, A. G.; Bowman, M. K.; Dzuba, S. A. Electron spin echo envelope modulation of molecular motions of deuterium nuclei. *J. Magn. Reson.* **2015**, *261*, 169−174.

(12) De Simone, F.; Guzzi, R.; Sportelli, L.; Marsh, D.; Bartucci, R. Electron spin-echo studies of spin-labelled lipid membranes and free fatty acids interacting with human serum albumin. *Biochim. Biophys. Acta, Biomembr.* **2007**, *1768*, 1541−1549.

(13) Dzuba, S. A. Structural studies of biological membranes using eseem spectroscopy of spin labels and deuterium substitution. *J. Struct. Chem.* **2013**, *54*, 1−15.

(14) Bottorf, L.; Rafferty, S.; Sahu, I. D.; McCarrick, R. M.; Lorigan, G. A. Utilizing electron spin echo envelope modulation to distinguish between the local secondary structures of an α-helix and an amphipathic 3_{10}helical peptide. *J. Phys. Chem. B* **2017**, *121*, 2961−2967.

(15) Sankararamakrishnan, R.; Adcock, C.; Sansom, M. S. P. The pore domain of the nicotinic acetylcholine receptor: molecular modeling, pore dimensions, and electrostatics. *Biophys. J.* **1996**, *71*, 1659−1671.

(16) Britt, R. D.; Lorigan, G. A.; Sauer, K.; Klein, M. P.; Zimmermann, J. L. The g = 2 multiline epr signal of the s_2 state of the photosynthetic oxygen-evolving complex originates from a ground spin state. *Biochim. Biophys. Acta, Bioenerg.* **1992**, *1140*, 95−101.

(17) Opella, S. J.; Marassi, F. M.; Gesell, J. J.; Valente, A. P.; Kim, Y.; Oblatt-Montal, M.; Montal, M. Structures of the M2 channel-lining segments from nicotinic acetylcholine and NMDA receptors by NMR spectroscopy. *Nat. Struct. Biol.* **1999**, *6*, 374−379.

(18) Chandrudu, S.; Simerska, P.; Toth, I. Chemical methods for peptide and protein production. *Molecules* **2013**, *18*, 4373−4388.

(19) Gongora-Benitez, M.; Tulla-Puche, J.; Albericio, F. Handles for Fmoc solid-phase synthesis of protected peptides. *ACS Comb. Sci.* **2013**, *15*, 217−228.

(20) Made, V.; Els-Heindl, S.; Beck-Sickinger, A. G. Automated solid-phase peptide synthesis to obtain therapeutic peptides. *Beilstein J. Org. Chem.* **2014**, *10*, 1197−1212.

(21) Inbaraj, J. J.; Cardon, T. B.; Laryukhin, M.; Grosser, S. M.; Lorigan, G. A. Determining the topology of integral membrane peptides using EPR spectroscopy. *J. Am. Chem. Soc.* **2006**, *128*, 9549−9554.

(22) Mayo, D. J.; Inbaraj, J. J.; Subbaraman, N.; Grosser, S. M.; Chan, C. A.; Lorigan, G. A. Comparing the structural topology of integral and peripheral membrane proteins utilizing electron paramagnetic resonance spectroscopy. *J. Am. Chem. Soc.* **2008**, *130*, 9656−9657.

(23) Urban, L.; Steinhoff, H. J. Hydrogen bonding to the nitroxide of protein bound spin labels. *Mol. Phys.* **2013**, *111*, 2873−2881.

(24) Bartucci, R.; Guzzi, R.; Sportelli, L.; Marsh, D. Intramembrane water associated with TOAC spin-labeled alamethicin: electron spin-echo envelope modulation by D2O. *Biophys. J.* **2009**, *96*, 997−1007.

(25) Milov, A. D.; Samoilova, R. I.; Shubin, A. A.; Gorbunova, E. Y.; Mustaeva, L. G.; Ovchinnikova, T. V.; Raap, J.; Tsvetkov, Y. D. Self-aggregation and orientation of the ion channel-forming zervamicin IIa in the membranes of ePC vesicles studied by cw EPR and ESEEM spectroscopy. *Appl. Magn. Reson.* **2010**, *38*, 75−84.

(26) Kumaresan, R.; Tufts, D. W. Estimating the parameters of exponentially damped sinusoids and pole-zero modeling in noise. *IEEE Trans. Acoust., Speech, Signal Process.* **1982**, *30*, 833−840.

(27) Columbus, L.; Kalai, T.; Jeko, J.; Hideg, K.; Hubbell, W. L. Molecular motion of spin labeled side chains in alpha-helices: Analysis by variation of side chain structure. *Biochemistry* **2001**, *40*, 3828−3846.

(28) Columbus, L.; Hubbell, W. L. A new spin on protein dynamics. *Trends Biochem. Sci.* **2002**, *27*, 288−295.
(29) Marchetto, R.; Schreier, S.; Nakaie, C. R. A novel spin-labeled amino-acid derivative for use in peptide-synthesis - (9-fluroenylmethyloxycarbonyl)-2,2,6,6-tetramethylpiperidine-n-oxyl-4-amino-4-carboxylic acid. *J. Am. Chem. Soc.* **1993**, *115*, 11042−11043.
(30) Sezer, D.; Freed, J. H.; Roux, B. Parametrization, molecular dynamics simulation, and calculation of electron spin resonance spectra of a nitroxide spin label on a polyalanine alpha-helix. *J. Phys. Chem. B* **2008**, *112*, 5755−5767.
(31) Batchelder, L. S.; Sullivan, C. E.; Jelinski, L. W.; Torchia, D. A. Characterization of leucine side-chain reorientation in collagen-fibrils by solid-state 2H NMR. *Proc. Natl. Acad. Sci. U. S. A.* **1982**, *79*, 386−389.
(32) Moore, C. R.; Yates, J. R.; Griffin, P. R.; Shabanowitz, J.; Martino, P. A.; Hunt, D. F.; Cafiso, D. S. Proteolytic fragments of the nicotinic acetylcholine-receptor identified by mass-spectrometry - implications for receptor topography. *Biochemistry* **1989**, *28*, 9184−9191.
(33) Liu, W.; Crocker, E.; Siminovitch, D. J.; Smith, S. O. Role of side-chain conformational entropy in transmembrane helix dimerization of glycophorin A. *Biophys. J.* **2003**, *84*, 1263−1271.
(34) Karpen, M. E.; de Haseth, P. L.; Neet, K. E. Differences in the amino acid distributions of 3 (10)- helices and alpha-helices. *Protein Sci.* **1992**, *1*, 1333−1342.
(35) Long, J. R.; Mills, F. D.; Raucci, F. A high resolution structure of the putative hinge region in M2 channel-lining segments of the nicotinic acetylcholine receptor. *Biochim. Biophys. Acta, Biomembr.* **2007**, *1768*, 2961−2970.
(36) Tikhonov, D. B.; Zhorov, B. S. Kinked-helices model of the nicotinic acetylcholine receptor ion channel and its complexes with blockers: simulation by the monte carlo minimization method. *Biophys. J.* **1998**, *74*, 242−255.
(37) Bransburg-Zabary, S.; Kessel, A.; Gutman, M.; Ben-Tal, N. Stability of an ion channel in lipid bilayers: Implicit solvent model calculations with gramicidin. *Biochemistry* **2002**, *41*, 6946−6954.
(38) Kessel, A.; Haliloglu, T.; Ben-Tal, N. Interactions of the M2delta segment of the acetylcholine receptor with lipid bilayers: a continuum-solvent model study. *Biophys. J.* **2003**, *85*, 3687−95.
(39) Kessel, A.; Shental-Bechor, D.; Haliloglu, T.; Ben-Tal, N. Interactions of hydrophobic peptides with lipid bilayers: monte carlo simulations with M2delta. *Biophys. J.* **2003**, *85*, 3431−44.

DOI: 10.1021/acs.jpcb.7b11890
J. Phys. Chem. B 2018, 122, 4388−4396